

See discussions, stats, and author profiles for this publication at: <https://www.researchgate.net/publication/49855332>

# Room-Temperature Fabrication of Ultrathin Oxide Gate Dielectrics for Low-Voltage Operation of Organic Field-Effect Transistors

ARTICLE *in* ADVANCED MATERIALS · FEBRUARY 2011

Impact Factor: 17.49 · DOI: 10.1002/adma.201003641 · Source: PubMed

---

CITATIONS

45

---

READS

70

## 4 AUTHORS, INCLUDING:



**Young Min Park**

Stanford University

9 PUBLICATIONS 197 CITATIONS

SEE PROFILE



**Martin Heeney**

Imperial College London

259 PUBLICATIONS 11,142 CITATIONS

SEE PROFILE

# Room-Temperature Fabrication of Ultrathin Oxide Gate Dielectrics for Low-Voltage Operation of Organic Field-Effect Transistors

Young Min Park, Jürgen Daniel, Martin Heeney, and Alberto Salleo\*

Organic field-effect transistors (OFETs) are attractive building blocks for low-cost electronic devices such as radio-frequency identification (RFID) tags, sensors, electronic paper, and back-plane circuits for active-matrix displays.<sup>[1–6]</sup> Low-voltage operation of OFETs is necessary for practical applications, hence the need to develop gate dielectrics with a high areal capacitance.<sup>[7,8]</sup> To this end, ultrathin dielectric layers have been demonstrated based on self-assembled-monolayer (SAM) chemistry.<sup>[7,9–11]</sup> In these cases, the formation of the dielectric layer relies on specific surface chemistries and therefore these approaches may not be suitable for the deposition of blanket layers on arbitrary substrates. For the same reason, the robustness and yield may be problematic due to the critical roles that surface cleanliness and roughness play on binding. On the other hand, inorganic, high- $\kappa$  metal oxide dielectrics, which are attractive due to their high dielectric constant, have been fabricated by various methods such as metal anodization,<sup>[10,12]</sup> vacuum-based deposition,<sup>[13–15]</sup> and sol-gel chemistry.<sup>[16]</sup> An advantage of an oxide dielectric is the ability to functionalize the surface with a variety of SAMs that are often found to be beneficial to charge transport in OFETs, or can be used to control the threshold voltage. Although inorganic/SAM hybrid dielectrics provide high capacitance and low leakage current, so far they have either required vacuum processing or relatively high-temperature anneals ( $T > 200$  °C), making them incompatible with low-cost solution processing on flexible substrates. Here, we describe the fabrication of low-voltage polymeric OFETs where the dielectric and the semiconductor are deposited from solution at room temperature. Zirconium oxide ( $\text{ZrO}_x$ ) was deposited via a sol-gel process and fully cured by UV irradiation under ambient conditions, eliminating the need for a high-temperature anneal. In order to reduce the leakage current and make the dielectric compatible with organic semiconductors,

the  $\text{ZrO}_x$  film was functionalized with a layer of octadecylphosphonic acid (ODPA). As a result, a high-performance ( $\mu = 0.2 \text{ cm}^2 \text{ V}^{-1} \text{ s}^{-1}$ ), low-voltage ( $|V_{\text{GS}}| < 3 \text{ V}$ ), and high-on-off-ratio ( $10^5$ – $10^6$ ) polymer OFET processed entirely from solution at room temperature is demonstrated using poly(2,5-bis(3-tetradecylthiophen-2-yl)thieno[3,2-b]thiophene) (PBTTC- $\text{C}_{14}$ ) as the semiconductor. The field-effect mobility was exclusively limited by the fact that the processing occurred entirely at room temperature and therefore the semiconductor was not annealed into its most-ideal microstructure.<sup>[17–19]</sup>

A staggered, bottom-gate device structure was fabricated (Figure 1a) using  $\text{ZrO}_x$  as the gate dielectric, due to its high dielectric constant ( $\kappa = 25$ ) and wide bandgap ( $E_g = 5.8 \text{ eV}$ ).<sup>[20]</sup> Typical  $\text{ZrO}_x$ -deposition methods include atomic-layer deposition,<sup>[21]</sup> sputtering,<sup>[22]</sup> and e-beam evaporation.<sup>[23]</sup> These methods, however, require vacuum and/or thermal anneals, which can result in higher processing costs and incompatibility with flexible substrates. We deposited the dielectric by an alternative method based on sol-gel chemistry. A zirconium(IV) acetylacetonate ( $\text{Zr}(\text{acac})_4$ ) solution in *N,N*-dimethylformamide (DMF) was spin-coated on a Si wafer and cured under a UV lamp, without the need for a high-temperature anneal.<sup>[16]</sup> The irradiation time was only limited by the power of the UV lamp available. The cured  $\text{ZrO}_x$  film was passivated with a layer of ODPA deposited from an isopropyl alcohol solution. To the best of our knowledge, this is the first demonstration of the fabrication of an ultrathin  $\text{ZrO}_x$  dielectric, processed from solution at room temperature.

X-ray photoelectron spectroscopy (XPS) was used to characterize compositional changes of the film deposited from  $\text{Zr}(\text{acac})_4$  solution upon UV irradiation (Figure 1b). In the as-spun sol-gel film, carbon and nitrogen due to the precursor and the solvent were detected. After UV irradiation for 15 min, the film did not contain any carbon and nitrogen and had an XPS spectrum similar to that of a thermally annealed (400 °C, 1 h) sol-gel  $\text{ZrO}_x$  film. The only species detected by XPS in the UV-irradiated film were Zr and O, in an approximate atomic ratio of 1:2. Atomic force microscopy (AFM) indicated that, after irradiation, the surface of the  $\text{ZrO}_x$  was smooth and uniform (Figure 1c). The roughness of the film, 0.22 nm, is comparable to commercial, thermally grown  $\text{SiO}_2$ .

Transmission electron microscopy showed the structure of the dielectric stack on Si after UV irradiation for 1.5 h (Figure 2a). The thickness of the  $\text{ZrO}_x$  layer was 6.3 nm; a 4.3 nm interface layer between the  $\text{ZrO}_x$  and the Si substrate was also visible. The interface layer measured in the UV-irradiated stack was thicker than that found in thermally annealed stacks (3 nm) or

Y. M. Park, Prof. A. Salleo  
Department of Materials Science and Engineering  
Stanford University  
Stanford, California 94305, USA  
E-mail: asalleo@stanford.edu

Dr. J. Daniel  
Palo Alto Research Center  
3333 Coyote Hill Road, Palo Alto, California 94304, USA  
Prof. M. Heeney  
Department of Chemistry  
Imperial College of London  
South Kensington Campus, London SW7 2AZ, UK

DOI: 10.1002/adma.201003641

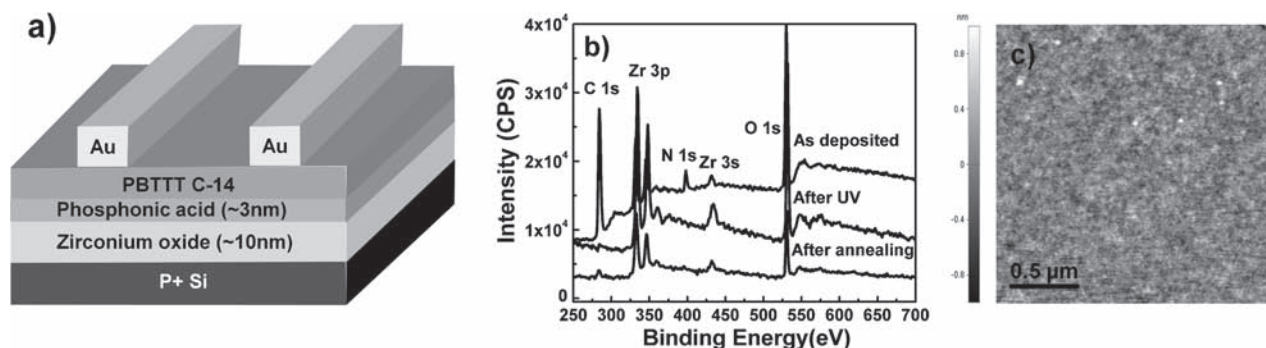


**Figure 1.** a) Top-contact device structure of OFETs fabricated on ultrathin hybrid dielectrics. b) X-ray photoelectron spectroscopy (XPS) analysis showing the compositional change of zirconium-based sol-gel films under UV irradiation and annealing. c) Atomic force microscopy (AFM) noncontact-mode topography of the UV-irradiated sol-gel  $\text{ZrO}_x$  film. The scale is  $2 \mu\text{m} \times 2 \mu\text{m}$ ; the height color scale is 0 to 2 nm (rms roughness: 0.22 nm)

native oxide (<2 nm). This observation suggests that during UV curing, oxygen diffuses through the stack and oxidizes the Si at the Si/ $\text{ZrO}_x$  interface.<sup>[24]</sup>

The capacitances of the bare  $\text{ZrO}_x$  cured for 90 and 60 min were, respectively,  $522 \text{ nF cm}^{-2}$  and  $470 \text{ nF cm}^{-2}$  at 50 Hz (Figure 2b). The thickness of the  $\text{ZrO}_x$ , as measured by ellipsometry, decreased as a function of irradiation time (inset in Figure 2b). Hence, the capacitance increase from 60 to 90 min irradiation was attributed to a slow densification process taking place during the UV irradiation. The formation of the dense  $\text{ZrO}_x$  film can be explained by the combination of two mechanisms: a relatively fast photolysis of the precursor by the UV irradiation and a slower densification of the film due to oxidation by a reactive oxygen species, possibly ozone. Photoexcitation of the precursor,  $\text{Zr}(\text{acac})_4$ , led to a ligand-to-metal charge transfer followed by decomposition into zirconium and organic ligands. Similar photolysis reactions under UV irradiation have been reported with other metal precursors.<sup>[25,26]</sup> The organic ligands and the residual solvent were successively oxidized into volatile gases. The light from the UV lamp used included UVV, corresponding the wavelength range of 100–185 nm; photolysis of ambient  $\text{O}_2$  during the UV irradiation, on the other hand, produces reactive oxygen species that adsorb on the  $\text{ZrO}_x$  film, react with Zr dangling bonds, and fill oxygen vacancies.<sup>[27]</sup> As

a result, the thickness of the dielectric gradually reduced with increasing UV-irradiation time. The observation that UV irradiation for 15 min removed all of the carbon and nitrogen from the film, yet did not produce a functional  $\text{ZrO}_x$  film with high dielectric constant and low loss corroborates a relatively fast photolysis followed by a slow densification. Indeed, low-power UV irradiation did not produce functional  $\text{ZrO}_x$  capacitors either. Assuming that the interface layer between the  $\text{ZrO}_x$  and Si was  $\text{SiO}_2$ , the calculated dielectric constant for UV-cured  $\text{ZrO}_x$  was estimated between 9.5 and 10.5. This value is lower than the reported value for crystalline  $\text{ZrO}_2$ .<sup>[20]</sup> The lower capacitance is probably due to the microstructure of the  $\text{ZrO}_x$ , which is a mixture of crystalline and amorphous oxides.

Chemical passivation of the dielectric further reduced the capacitance of the dielectric stacks ( $320 \text{ nF cm}^{-2}$  at 50 Hz for the  $\text{ZrO}_x$  cured for 1.5 h) because of the introduction of the low-permittivity ODPA layer. The ODPA treatment, however, dramatically lowered the leakage current through the capacitor from  $1.76 \times 10^{-4} \text{ A cm}^{-2}$  at an applied voltage of  $-3 \text{ V}$  to  $3.88 \times 10^{-7} \text{ A cm}^{-2}$ , and increased the breakdown voltage beyond 4 V on both the positive- and negative-bias sides (Figure 2c). An ODPA layer affects the leakage-current density and the breakdown voltage beneficially, thanks to its long insulating alkyl chains.<sup>[10,28]</sup> It is important to note that the reduced leakage

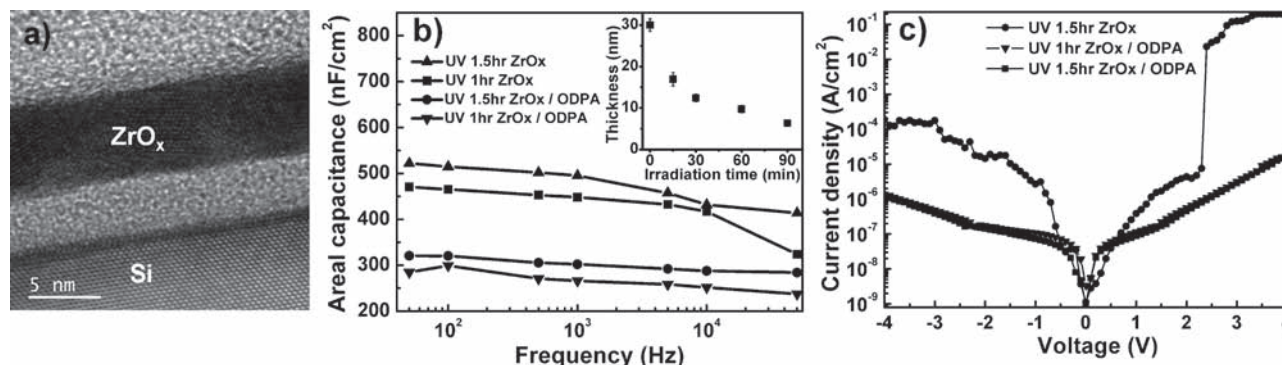


**Figure 2.** a) Cross-sectional TEM image of the dielectric stack on Si. b) Areal capacitance as a function of frequency. The thickness change of as-deposited  $\text{ZrO}_x$  with UV-irradiation time is shown in the inset. To calculate the  $\text{ZrO}_x$  thickness,  $\text{SiO}_2$  interlayer thickness values of 4 nm and 2 nm were used and the results were averaged. c) Leakage-current density as a function of bias voltage measured on the dielectric stacks processed for different times under UV and with or without ODPA.

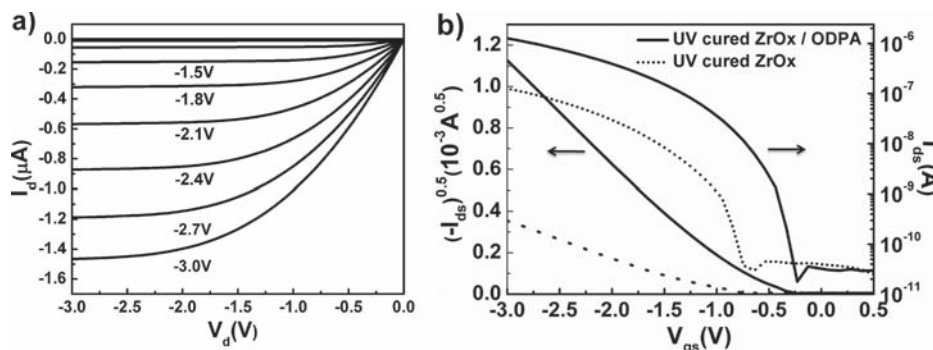


**Figure 3.** a) Output curve of PBTTT-C<sub>14</sub> OFETs on ZrO<sub>x</sub>/ODPA (irradiation time = 90 min). b) Transfer curves of OFETs on ZrO<sub>x</sub>, with and without ODPA, measured at  $V_{DS} = -1.5$  V.

current was essentially caused by the ODPA treatment, and not by the high-bandgap interface layer assumed to be SiO<sub>2</sub> ( $E_g = 8.9$  eV), which indicates that this hybrid dielectric was compatible with other metal substrates. Preliminary results indicate that the UV-cured ZrO<sub>x</sub> can also be used as a dielectric on patterned gate electrodes. In summary, the ODPA-treated, UV-cured ZrO<sub>x</sub> dielectric is suitable for low-voltage operation of both p and n-type OFETs.

PBTTT OFETs processed on UV-irradiated ZrO<sub>x</sub> with and without ODPA were well behaved (Figure 3a,b). The OFET fabricated on bare ZrO<sub>x</sub> displayed a subthreshold swing of  $150 \text{ mV dec}^{-1}$ , an onset voltage of  $-0.75$  V, and on-off current ratio of  $10^4$ . Following passivation with ODPA, the subthreshold swing decreased to  $110 \text{ mV dec}^{-1}$  and the onset voltage was lowered to  $-0.25$  V; the transistor reached an on-off swing of  $10^5$  within a gate voltage interval of 3 V. The device improvement is compatible with a reduction in interfacial trap states due to the passivation of the surface hydroxyl groups on the inorganic oxide.<sup>[29,30]</sup> Gate currents of the order of 0.1 nA could be partially attributed to the unpatterned, heavily doped Si gate electrode. The presence of ODPA also improved the carrier mobility of the PBTTT from  $0.016$  to  $0.18 \text{ cm}^2 \text{ V}^{-1} \text{ s}^{-1}$ , as previously reported for devices processed on silane-treated SiO<sub>2</sub>.<sup>[31,32]</sup> The performance of the semiconductor on our dielectric stack is identical to that obtained on silane-treated SiO<sub>2</sub>, further highlighting the high quality of the ZrO<sub>x</sub>/ODPA combination.<sup>[32]</sup> Furthermore, the low-permittivity passivation layer may weaken the interaction between the charge carriers and the high-polarizability dielectric, which is believed to cause a lowering of the mobility of organic semiconductors on high- $\kappa$  dielectrics.<sup>[33,34]</sup>

In conclusion, we have demonstrated the solution-based fabrication of low-voltage OFETs entirely at room temperature and without the use of vacuum deposition. We used a hybrid dielectric composed of a high- $\kappa$  dielectric layer (ZrO<sub>x</sub>) deposited from solution and cured by UV irradiation combined with a phosphonic acid passivation layer. The performance of these organic thin-film transistors (OTFTs) is identical to that of state-of-the-art devices fabricated on silane-treated thermal SiO<sub>2</sub>. Operation in a 3 V range, with on-off ratios of the order of  $10^5$  and a carrier mobility of  $0.18 \text{ cm}^2 \text{ V}^{-1} \text{ s}^{-1}$  were obtained using PBTTT-C<sub>14</sub> as a semiconductor. The development of a high-capacitance dielectric layer, processed at room temperature, is of interest as organic transistors move towards applications.

## Experimental Section

**Zirconium Oxide and Phosphonic Acid Self-Assembled-Monolayer Preparation:** Prime-grade, heavily p-doped silicon wafers (100) were used as the substrate. Before the deposition of the sol-gel solution, the substrates were sonicated in acetone, methanol, and isopropyl alcohol, and cleaned in a UV ozone cleaner for 20 min each. Zirconium oxide sol-gel solution was synthesized by dissolving Zr(IV) acetylacetonate ( $\text{Zr}(\text{C}_5\text{H}_7\text{O}_2)_4$ ) (98% Sigma-Aldrich) in 5 ml of *N,N*-dimethylformamide ( $\text{C}_3\text{H}_7\text{NO}$ ) (Sigma-Aldrich) at a concentration of 0.1 M under a nitrogen atmosphere with the addition of an equimolar concentration of ethanolamine ( $\text{C}_2\text{H}_7\text{NO}$ ) (Sigma-Aldrich). The solution was stirred and kept at  $70^\circ\text{C}$  for 3 h to enhance hydrolysis. The zirconium oxide gel film was formed by spin-coating  $100 \mu\text{l}$  at 5 000 rpm for 60 s on a piece of the heavily doped p-type Si,  $1.5 \text{ cm} \times 1.5 \text{ cm}$  in size, to form a 30 nm gel film. In order to photolyze and densify the film, the sample was cured under a high-pressure mercury UV lamp including the wavelengths of UVA, UVB and UVV at  $270 \text{ mW cm}^{-2}$  in atmosphere and at room temperature. After UV irradiation, the thickness of the ZrO<sub>x</sub> film was 6–7 nm (measured by TEM). As a comparison, the as-deposited films were annealed at  $400^\circ\text{C}$  under a nitrogen atmosphere for 1 h, then cooled to room temperature.

A phosphonic acid self-assembled monolayer was deposited on the cured ZrO<sub>x</sub> dielectric by immersion in a  $5 \times 10^{-3} \text{ M}$  *n*-octadecylphosphonic acid solution in 2-propanol. The substrates were left in solution at room temperature for about 4 h and successively sonicated in pure 2-propanol for 10 min, blown dry with nitrogen, and briefly baked on a hot plate at  $60^\circ\text{C}$ . The thickness of the ODPA self-assembled monolayer was 3.1 nm, as measured using TEM, and the contact angle with water was  $102^\circ$ .

**Device Fabrication and Characterization:** All of the transistors and capacitors were measured in air. For the OFETs, poly(2,5-bis(3-tetradecylthiophen-2-yl)thieno[3,2-b]thiophene) (PBTTT-C<sub>14</sub>) ( $M_n = 22\,000 \text{ g mol}^{-1}$ ;  $M_w = 44\,000 \text{ g mol}^{-1}$ ) was deposited by spin-coating from 0.5 wt% solutions in 1,2-dichlorobenzene on phosphonic acid/ZrO<sub>x</sub>/heavily doped Si substrate. Top-contact, Au source and drain electrodes (thickness = 100 nm) were deposited by thermal evaporation through a shadow mask to define a channel length of  $60 \mu\text{m}$ . The channel width ( $500 \mu\text{m}$ ) was defined by isolating single devices. The field-effect mobility was calculated in the saturation regime. The threshold voltage was extracted from the intercept of the  $(-I_d)^{0.5}$  vs  $V_g$  curve with the  $V_g$  axis. To define the capacitors, a square pattern of Al with an area of  $0.012 \text{ cm}^2$  was thermally evaporated on the dielectric. The capacitance measurements were performed using an HP 4284 LCR meter at frequencies ranging from 50 Hz to 50 kHz. The capacitance value measured at 50 Hz was used to extract the mobility. TEM characterization was performed using an FEI Tecnai G2 F20 instrument. Cross-sectional TEM samples were prepared using conventional methods (polishing and ion milling). Noncontact-AFM characterization was performed on a Park Systems XE-70 scanning probe microscope. Chemical-element analysis was performed using a PHI Versa Probe Scanning XPS Microprobe.



## Acknowledgements

Y.M.P. was supported by a Thomas V. Jones Stanford Graduate Fellowship. A.S. gratefully acknowledges support from Toshiba Corporation through the Center for Integrated Systems at Stanford University. Y.M.P. thanks Dr. B. Shin and Dr. J. H. Lim for helpful discussions. The authors thank Professor P. C. McIntyre for use of the LCR meter.

Received: October 19, 2010

Published online: January 13, 2011

- [1] C. Dimitrakopoulos, P. Malenfant, *Adv. Mater.* **2002**, *14*, 99.
- [2] S. R. Forrest, *Nature* **2004**, *428*, 911.
- [3] T. Kelley, P. Baude, C. Gerlach, D. Ender, D. Muires, M. Haase, D. Vogel, S. Theiss, *Chem. Mater.* **2004**, *16*, 4413.
- [4] M. E. Roberts, S. C. B. Mannsfeld, N. Queraltó, C. Reese, J. Locklin, W. Knoll, Z. Bao, *Proc. Natl. Acad. Sci. USA* **2008**, *105*, 12134.
- [5] H. Sirringhaus, *Adv. Mater.* **2005**, *17*, 2411.
- [6] T. Someya, T. Sekitani, S. Iba, Y. Kato, H. Kawaguchi, T. Sakurai, *Proc. Natl. Acad. Sci. USA* **2004**, *101*, 9966.
- [7] A. Facchetti, M.-H. Yoon, T. J. Marks, *Adv. Mater.* **2005**, *17*, 1705.
- [8] R. P. Ortiz, A. Facchetti, T. J. Marks, *Chem. Rev.* **2009**, *110*, 205.
- [9] M. Halik, H. Klauk, U. Zschieschang, G. Schmid, C. Dehm, M. Schutz, S. Maisch, F. Effenberger, M. Brunnbauer, F. Stellacci, *Nature* **2004**, *431*, 963.
- [10] H. Klauk, U. Zschieschang, J. Pflaum, M. Halik, *Nature* **2007**, *445*, 745.
- [11] M.-H. Yoon, A. Facchetti, T. J. Marks, *Proc. Natl. Acad. Sci. USA* **2005**, *102*, 4678.
- [12] L. A. Majewski, R. Schroeder, M. Grell, *Adv. Mater.* **2005**, *17*, 192.
- [13] X.-H. Zhang, B. Domercq, X. Wang, S. Yoo, T. Kondo, Z. L. Wang, B. Kippelen, *Org. Electron.* **2007**, *8*, 718.
- [14] D. K. Hwang, C. S. Kim, J. M. Choi, K. Lee, J. H. Park, E. Kim, H. K. Baik, J. H. Kim, S. Im, *Adv. Mater.* **2006**, *18*, 2299.
- [15] Y. W. Choi, I. D. Kim, H. L. Tuller, A. I. Akinwande, *IEEE Trans. Electron Devices* **2005**, *52*, 2819.
- [16] O. Acton, G. Ting, H. Ma, J. W. Ka, H.-L. Yip, N. M. Tucker, A. K.-Y. Jen, *Adv. Mater.* **2008**, *20*, 3697.
- [17] M. L. Chabinyc, M. F. Toney, R. J. Kline, I. McCulloch, M. Heeney, *J. Am. Chem. Soc.* **2007**, *129*, 3226.
- [18] B. H. Hamadani, D. J. Gundlach, I. McCulloch, M. Heeney, *Appl. Phys. Lett.* **2007**, *91*, 243512.
- [19] I. McCulloch, M. Heeney, C. Bailey, K. Genevicius, I. MacDonald, M. Shkunov, D. Sparrowe, S. Tierney, R. Wagner, W. Zhang, *Nat. Mater.* **2006**, *5*, 328.
- [20] J. Robertson, *Rep. on Prog. in Phys.* **2006**, *69*, 327.
- [21] A. Javey, H. Kim, M. Brink, Q. Wang, A. Ural, J. Guo, P. McIntyre, P. McEuen, M. Lundstrom, H. Dai, *Nat. Mater.* **2002**, *1*, 241.
- [22] M. Zirkel, A. Haase, A. Fian, H. Schön, C. Sommer, G. Jakopic, G. Leising, B. Stadlober, I. Graz, N. Gaar, *Adv. Mater.* **2007**, *19*, 2241.
- [23] J.-M. Kim, J.-W. Lee, J.-K. Kim, B.-K. Ju, J.-S. Kim, Y.-H. Lee, M.-H. Oh, *Appl. Phys. Lett.* **2004**, *85*, 6368.
- [24] M. Copel, M. Gribelyuk, E. Gusev, *Appl. Phys. Lett.* **2000**, *76*, 436.
- [25] H. Park, D. Choi, X. Zhang, S. Jeon, S. Park, S. Lee, S. Kim, K. Kim, J. Choi, J. Lee, *J. Mater. Chem.* **2010**, *20*, 1921.
- [26] D. Versace, O. Soppera, J. Lalevée, C. Croutxé-Barghorn, *New J. Chem.* **2008**, *32*, 2270.
- [27] I. Boyd, J. Zhang, *Solid-State Electron.* **2001**, *45*, 1413.
- [28] K. Fukuda, T. Hamamoto, T. Yokota, T. Sekitani, U. Zschieschang, H. Klauk, T. Someya, *Appl. Phys. Lett.* **2009**, *95*, 203301.
- [29] A. Salleo, M. Chabinyc, M. Yang, R. Street, *Appl. Phys. Lett.* **2002**, *81*, 4383.
- [30] L.-L. Chua, J. Zaumseil, J.-F. Chang, E. C. W. Ou, P. K. H. Ho, H. Sirringhaus, R. H. Friend, *Nature* **2005**, *434*, 194.
- [31] R. J. Kline, D. M. DeLongchamp, D. A. Fischer, E. K. Lin, M. Heeney, I. McCulloch, M. F. Toney, *Appl. Phys. Lett.* **2007**, *90*, 062117.
- [32] C. Wang, L. H. Jimison, L. Goris, I. McCulloch, M. Heeney, A. Ziegler, A. Salleo, *Adv. Mater.* **2010**, *22*, 697.
- [33] I. N. Hulea, S. Fratini, H. Xie, C. L. Mulder, N. N. Iossad, G. Rastelli, S. Ciuchi, A. F. Morpurgo, *Nat. Mater.* **2006**, *5*, 982.
- [34] J. Veres, S. D. Ogier, S. W. Leeming, D. C. Cupertino, S. M. Khaffaf, *Adv. Funct. Mater.* **2003**, *13*, 199.